Supplemental Data

Resolvin T-series Reduce Neutrophil Extracellular Traps

Nan Chiang[1], Miyuki Sakuma[2], Ana R. Rodriguez[3], Bernd W. Spur[3], Daniel Irimia[2], Charles N. Serhan[1]

[1]Center for Experimental Therapeutics and Reperfusion Injury, Department of Anesthesiology, Perioperative and Pain Medicine, Brigham and Women's Hospital and Harvard Medical School, Boston, Massachusetts 02115, USA
[2]BioMEMS Resource Center, Center for Engineering in Medicine and Surgical Services, Massachusetts General Hospital, Shriners Hospital for Children, and Harvard Medical School, Boston, Massachusetts 02129, USA
[3]Department of Cell Biology and Neuroscience, Rowan University-SOM, Stratford, New Jersey 08084, USA.

Address correspondence and reprint requests to:
Prof. Charles N. Serhan, Director
Center for Experimental Therapeutics and Reperfusion Injury,
60 Fenwood Rd., Hale Building for Transformative Medicine 3-016, Boston,
Massachusetts 02115, USA.
Phone: 617-525-5001; Fax: 617-525-5017
E-mail: cserhan@bwh.harvard.edu

This PDF includes:

Supplemental Methods

Figure S1-S5

Supplemental Methods

MPO measurements

Human PMNs were adhered onto 12-well plates ($2x10^6$ cells/well) in NET buffer, incubated with RvT1 (10 nM) or vehicle control for 15 min, followed by addition of IL-1β (50 ng/ml) for 4 hours at 37°C. Cells were washed twice with PBS and then incubated with S7 micrococcal nuclease (15 units/ml/well; Thermo Fisher Scientific) in NET buffer for 30 min at 37°C to cleave NETs. Supernatants containing NETs were collected for MPO determinations (R&D Systems, DY3174) following manufacturer's protocol.

S. aureus infection in murine dorsal air pouch

Murine infectious exudates were collected. Total leukocyte counts were determined by light microscopy, and PMN percentages determined by differential counting using Wright-Giemsa stain kit (Thermo Scientific, Waltham, MA). For bacterial titers, aliquots of exudates were plated onto LB agar plates and cultured overnight at 37°C. For NET, exudate cells ($2x10^5$ cells) were incubated with Sytox Green (5 μM) for 10 min and loaded onto the microfluidic NET device for quantification. In parallel, exudate cells ($1x10^5$ cells) were adhered onto a 96-well plate, incubated with Sytox Green (5 μM) for 10 min and washed once with PBS. Fluorescence was determined using a SpectraMax M3 plate reader (Molecular Devices), and fluorescence of total DNA was determined following TritonX-100 lysis. Images were taken using a Keyence BZ-9000 (BIOREVO) inverted fluorescence phase-contrast microscope (20X objective) equipped with a monochrome/color switching camera using BZ-II Viewer software and BZ-II Analyzer (Keyence).

Preparation of human NETs for macrophage phagocytosis

Freshly isolated human PMNs were adhered onto 6-well plates ($10x10^6$ cells/well) in NET buffer and incubated with PMA (20 nM) with Sytox Green (5 μM) for 4 hours at 37°C. Supernatants were aspirated and cells washed twice with PBS. S7 micrococcal nuclease (15 units/ml; 2 ml/well) was then added for 30 min at 37°C to

cleave NETs. Supernatants containing NETs were collected and stored at -20°C. Approximately 100 μg DNA was obtained from $10x10^6$ PMN.

Immunofluorescence staining

Human PMNs ($2x10^5$ cells/well) were stained with Sytox Green (5 μM), fixed in 4% paraformaldehyde, and in some experiments, stained with PE-conjugated anti-human CD66b IgG (1:200 dilution; BD Biosciences). In select experiments, human MΦs (100,000 cells/well) with ingested NETs were stained with (1) PKH26 red (1:1000 dilution, Millipore Sigma, St. Louis, MO), or (2) anti-pAMPK IgG (1:100 dilution; Cell Signaling, Catalog No. 2535), followed by PE-conjugated anti-rabbit IgG (1:200; eBioscience). Mouse MΦs with ingested NETs were stained with PE-conjugated anti-F4/80 IgG (1:200; eBioscience). Mouse exudates ($2x10^5$ cells/well) were stained with Sytox Green (5 μM), fixed in 4% paraformaldehyde, then stained with (1) PE-conjugated anti-mouse Ly-6G IgG (clone 1A8, Biolegend, San Diego, CA), or (2) goat anti-mouse MPO IgG (1:100 dilutions; DY3667, R&D Systems), followed by Cy™3-conjugated Donkey anti-goat IgG (1:200 dilutions; cat no. 705-165-147, Jackson ImmunoResearch Laboratories, Inc., West Grove, Pennsylvania).

Human macrophage differentiation and proliferation

PBMCs were isolated by Ficoll-Histopaque-1077 density-gradient. Monocytes were adhered in PBS, and then cultured in complete RPMI-1640 medium (Lonza, NJ) containing 10% fetal calf serum and recombinant human GM-CSF (20 ng/ml; R&D Systems) for 7 days for macrophage (MΦ) differentiation to M0 phenotype. In select experiments, MΦ were polarized towards M1 and M2. Briefly, M1 MΦs were prepared from monocytes incubated with GM-CSF (20 ng/ml) for 7 days in RPMI-1640 medium, followed by LPS (100 ng/ml) and INF-γ (20 ng/ml) for 48 h. M2 was obtained by incubating monocytes with M-CSF (20 ng/ml) for 7 days followed by 20 ng/ml IL-4 for 48 h.

A

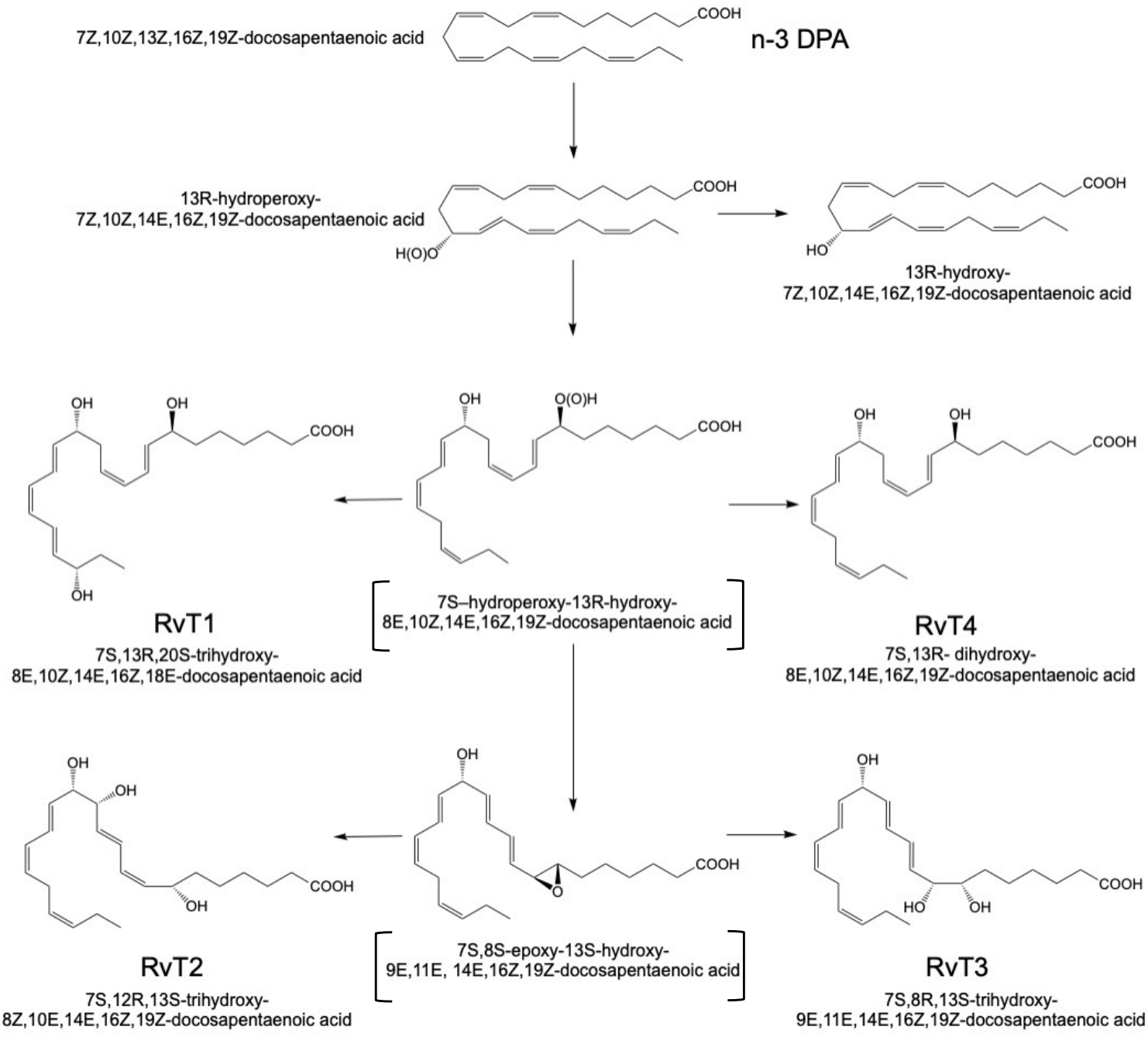
7Z,10Z,13Z,16Z,19Z-docosapentaenoic acid
n-3 DPA
13R-hydroperoxy-
7Z,10Z,14E,16Z,19Z-docosapentaenoic acid
13R-hydroxy-
7Z,10Z,14E,16Z,19Z-docosapentaenoic acid
7S–hydroperoxy-13R-hydroxy-
8E,10Z,14E,16Z,19Z-docosapentaenoic acid
RvT1
7S,13R,20S-trihydroxy-
8E,10Z,14E,16Z,18E-docosapentaenoic acid
RvT4
7S,13R- dihydroxy-
8E,10Z,14E,16Z,19Z-docosapentaenoic acid
7S,8S-epoxy-13S-hydroxy-
9E,11E, 14E,16Z,19Z-docosapentaenoic acid
RvT2
7S,12R,13S-trihydroxy-
8Z,10E,14E,16Z,19Z-docosapentaenoic acid
RvT3
7S,8R,13S-trihydroxy-
9E,11E,14E,16Z,19Z-docosapentaenoic acid

B

MS/MS

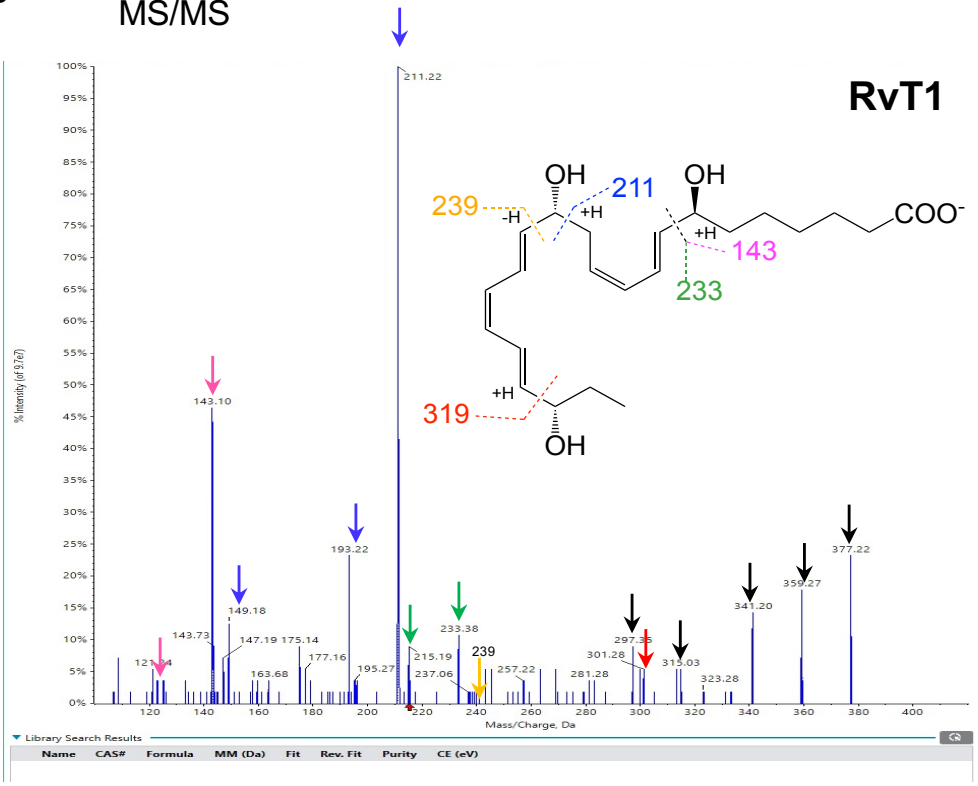

377=M-H
359=M-H-H_2O
341=M-H-2H_2O
315=M-H-H_2O-CO_2
301=319-H_2O
297=M-H-2H_2O-CO_2
215=233-H_2O
193=211-H_2O
149=211-H_2O-CO_2
125=143-H_2O

UV spectrum

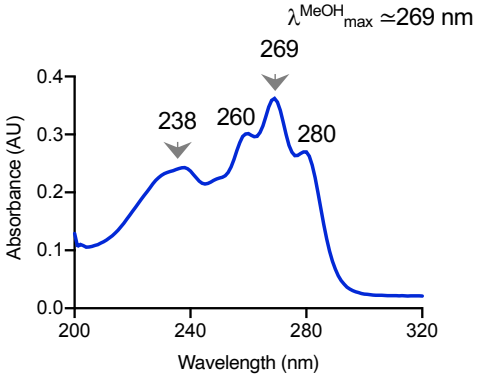

C

MS/MS

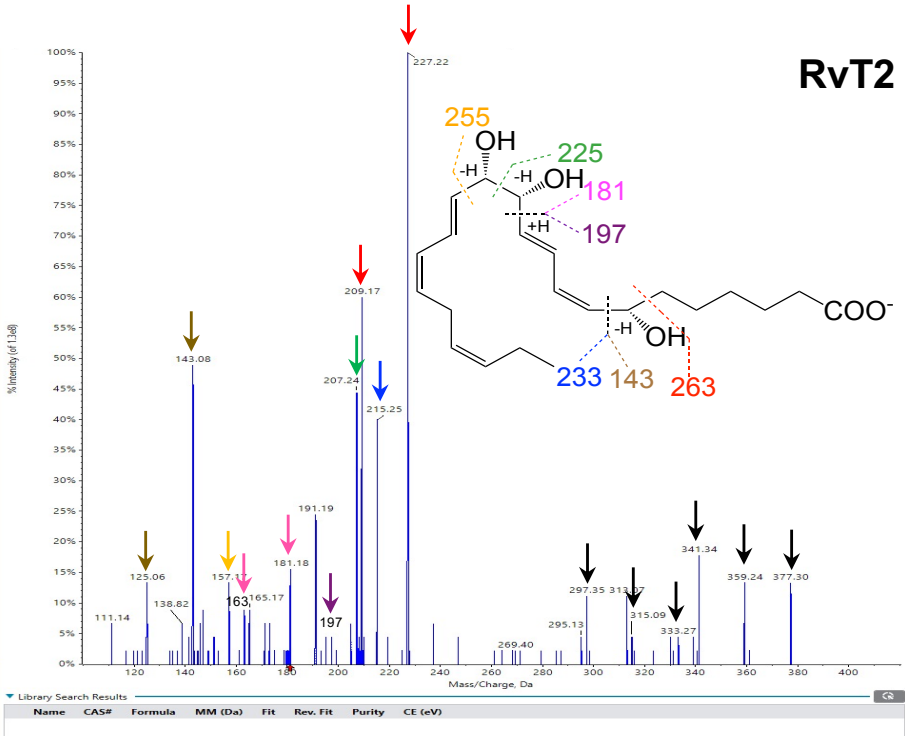

377=M-H
359=M-H-H_2O
341=M-H-2H_2O
333=M-H-CO_2
315=M-H-H_2O-CO_2
297=M-H-2H_2O-CO_2
227=263-2H_2O
209=263-3H_2O
207=225-H_2O
215=233-H_2O
163=181-H_2O
157=255-3H_2O-CO_2
125=143-H_2O

UV spectrum

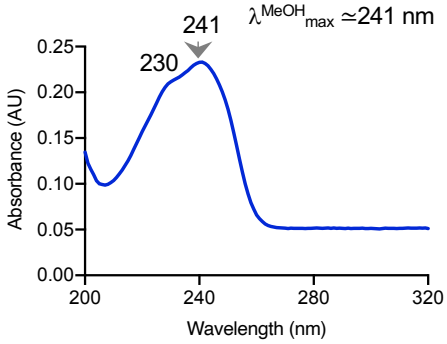

D

MS/MS

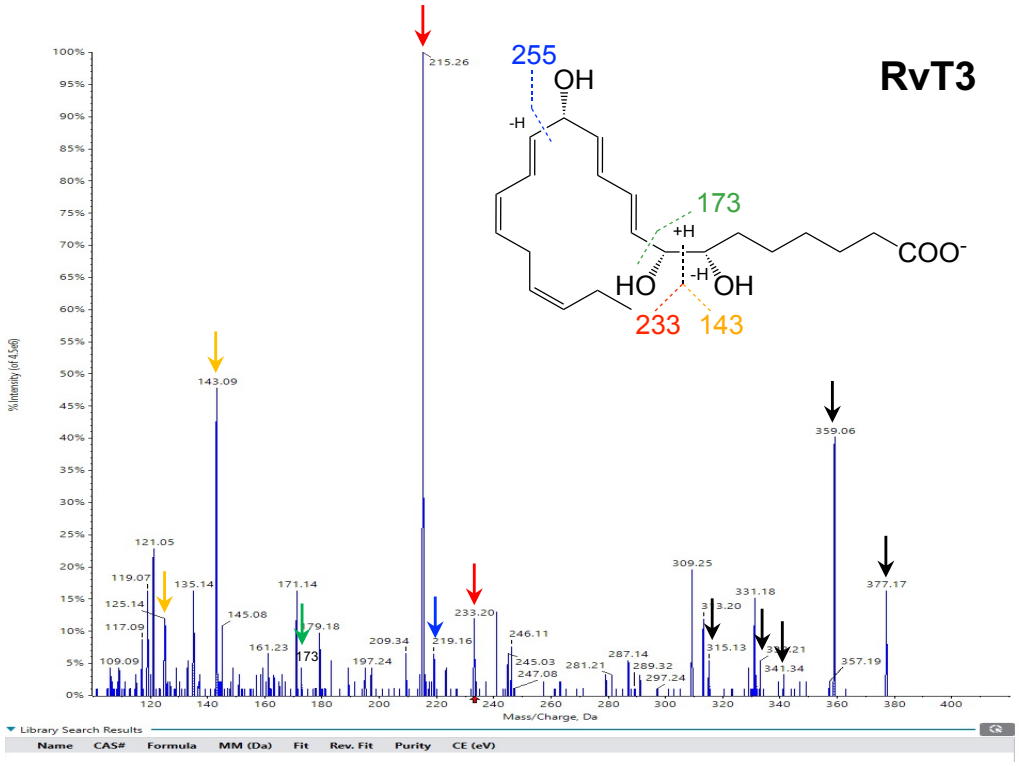

377=M-H
359=M-H-H_2O
341=M-H-2H_2O
333=M-H-CO_2
315=M-H-H_2O-CO_2
215=233-H_2O
219=255-2H_2O
125=143-H_2O

UV spectrum

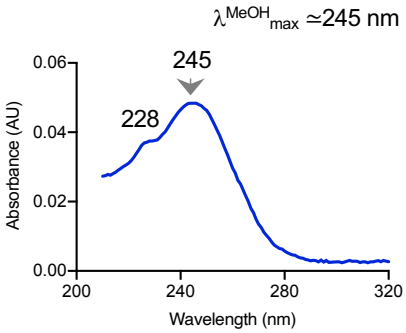

E

MS/MS

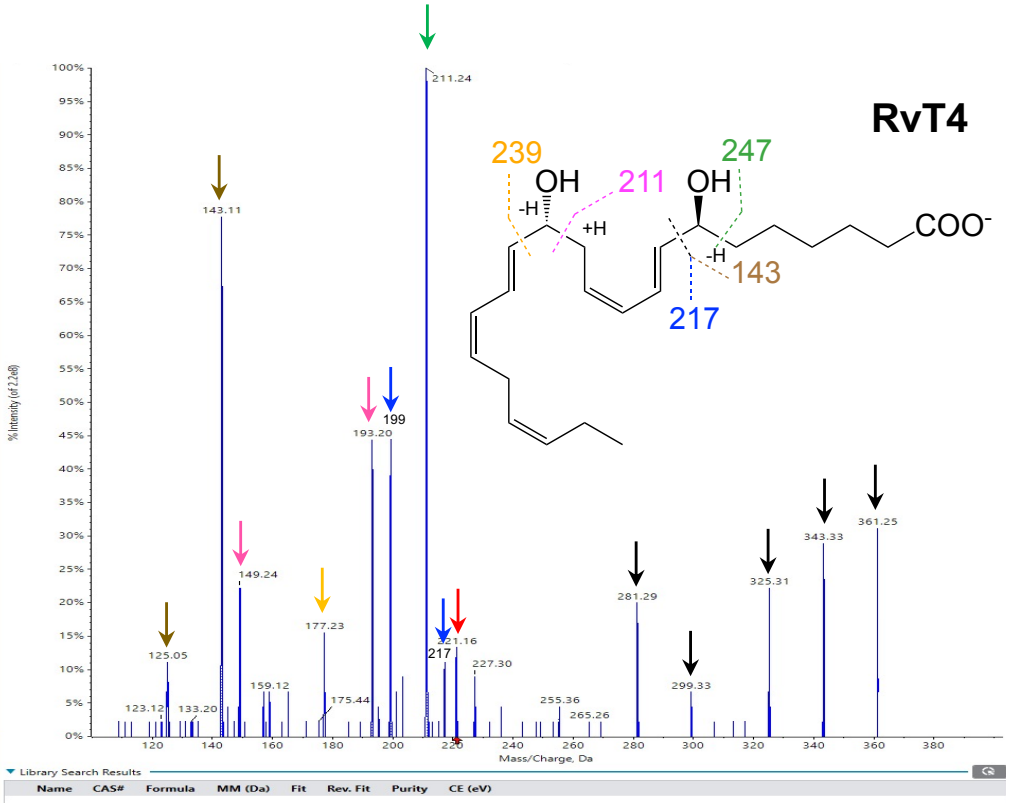

361=M-H
343=M-H-H_2O
325=M-H-2H_2O
299=M-H-H_2O-CO_2
281=M-H-2H_2O-CO_2
221=239-H_2O
211=247-2H_2O
199=217-H_2O
193=211-H_2O
149=211-H_2O-CO_2
177=239-H_2O-CO_2
125=143-H_2O

UV spectrum

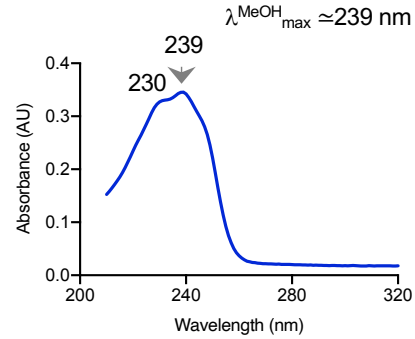

Figure S1. Proposed biosynthesis of RvTs, and authentication of synthetic RvTs.
(A) Proposed biosynthesis of RvTs. RvT biosynthesis is initiated by conversion of n-3 DPA (Dalli *et al.,* 2015) to the intermediate 13R-HpDPA (13R-Hydroperoxy-7Z,10Z,13R,14E,16Z,19Z docosapentaenoic acid). This intermediate was prepared by total organic synthesis and its conversion was proven to RvT1, RvT2, RvT3 and RvT4 with human neutrophils (Primdahl *et al*., 2016).

(B-E) MS/MS and UV spectra of RvT1, RvT2, RvT3 and RvT4.
Physical properties of each synthetic RvTs were examined and compared to published results for authentication (Dalli et al., 2015; Primdahl et al., 2016). LC-MS/MS was carried out in the negative ionization mode using a liquid chromatography-tandem linear ion trap quadrupole mass spectrometer system, QTRAP 6500+ (Sciex, Waltham, MA) equipped with a Sciex ExionLC (Sciex, Waltham, MA) as in Walker *et al*., 2021. A Kinetex Polar C18 LC column (100mm x 4.6mm x 2.6µm; Phenomenex, Torrance, CA) was kept in a column oven maintained at 50°C. The RvTs were each eluted with a gradient of water/methanol/formic acid 55:45:0.1 (v/v/v) to 20:80:0.1 from 2.0–16.5 min, then by 20:80:0.1 to 2:98:0.1 from 16.5–16.6 min, followed by an isocratic elution at 2:98:0.1 from 16.6–18.5 min, and finally 2:98:0.1 to 90:10:0.1 until 20.5 min at a 0.5 mL/min flow rate. A targeted multiple reaction monitoring (MRM) method was devised with signature ion fragments for each molecule.

(B) RvT1 MS/MS fragments: m/z 377=M-H, 359=M-H-H_2O, 341=M-H-2H_2O, 315=M-H-H_2O-CO_2, 301=319-H_2O, 297=M-H-2H_2O-CO_2, 239, 233, 215=233-H_2O, 193=211-H_2O, 149=211-H_2O-CO_2, 125=143-H_2O. For UV spectrum, RvT1 possesses a conjugated triene, that gave a UV chromophore with λ^{MeOH}_{max} ≃269 nm and shoulders ≃260 and 280 nm, RvT1 also has a conjugated diene, giving a λ^{MeOH}_{max} ≃238 nm.

(C) RvT2 MS/MS fragments : m/z 377=M-H, 359=M-H-H_2O, 341=M-H-2H_2O, 333=M-H-CO_2, 315=M-H-H_2O-CO_2, 297=M-H-2H_2O-CO_2, 227=263-2H_2O, 209=263-3H_2O, 207=225-H_2O, 215=233-H_2O, 197, 181, 163=181-H_2O, 157=255-3H_2O-CO_2, 143, 125=143-H_2O. For UV spectrum, RvT2 has double conjugated dienes, giving a UV chromophore with λ^{MeOH}_{max} ≃241 nm, and a shoulder ≃230 nm.

(D) RvT3 MS/MS fragments: m/z 377=M-H, 359=M-H-H_2O, 341=M-H-2H_2O, 333=M-H-CO_2, 315=M-H-H_2O-CO_2, 233, 215=233-H_2O, 219=255-2H_2O, 173, 143, 125=143-H_2O. For UV spectrum, RvT3 has double conjugated dienes, giving a UV chromophore with λ^{MeOH}_{max} ≃245 nm, and a shoulder ≃230 nm.

(E) RvT4 MS/MS fragments: m/z 361=M-H, 343=M-H-H_2O, 325=M-H-2H_2O, 299=M-H-H_2O-CO_2, 281=M-H-2H_2O-CO_2, 221=239-H_2O, 211=247-2H_2O, 199=217-H_2O, 193=211-H_2O, 149=211-H_2O-CO_2, 177=239-H_2O-CO_2, 143, 125=143-H_2O. For UV spectrum, RvT4 has double conjugated dienes, giving a UV chromophore with λ^{MeOH}_{max} ≃239 nm, and a shoulder ≃230 nm.

References:

Dalli, J., N. Chiang, and C.N. Serhan. 2015. Elucidation of novel 13-series resolvins that increase with atorvastatin and clear infections. *Nat. Med.* 21:1071-1075.

Primdahl, K.G., M. Aursnes, M.E. Walker, R.A. Colas, C.N. Serhan, J.Dalli, T.V. Hansen, A. Vik. 2016. Synthesis of 13(R)-Hydroxy-7Z,10Z,13R,14E,16Z,19Z Docosapentaenoic Acid (13R-HDPA) and Its Biosynthetic Conversion to the 13-Series Resolvins. *J Nat Prod*. 79:2693-2702.

Walker KH, Krishnamoorthy N, Brüggemann TR, Shay AE, Serhan CN, Levy BD. Protectins PCTR1 and PD1 Reduce Viral Load and Lung Inflammation During Respiratory Syncytial Virus Infection in Mice. Front Immunol. 2021 Aug 19;12:704427. doi: 10.3389/fimmu.2021.704427. PMID: 34489955; PMCID: PMC8417406.

A

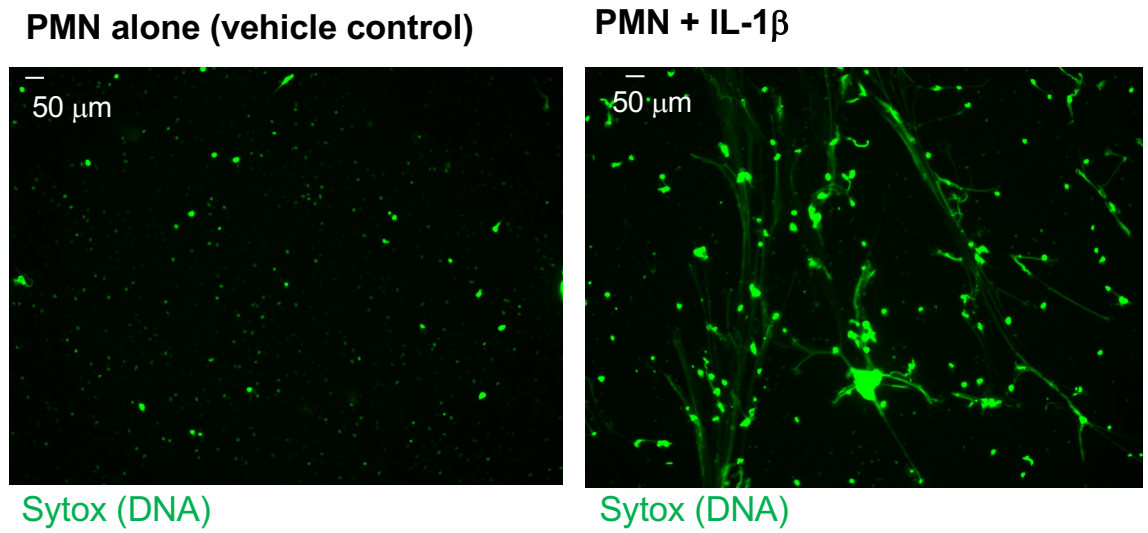

B

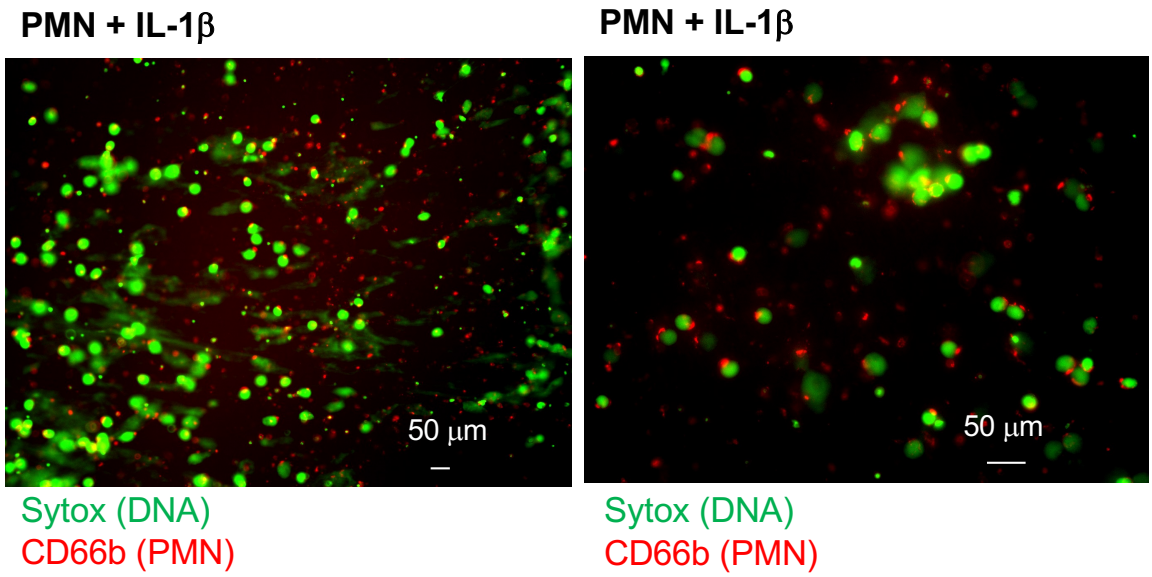

C

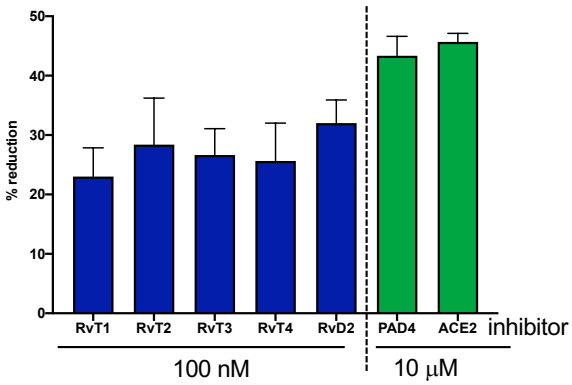

Figure S2. Human PMN NET formation and regulation by RvTs
See Methods and figure legend of Figure 3 for experimental details.
(A,B) Human PMNs were incubated with vehicle or IL-1β for 4h. Green: Sytox Green for DNA, red: anti-CD66b for human PMN. Scale bars: 50 μm.
(C) Comparisons of SPMs [100 nM] and a PAD4 inhibitor [10 μM]; mean±SEM; n=7 (SPM) or 3 (PAD4 inhibitor). No statistically significant differences were obtained using one-way ANOVA with Tukey's multiple comparisons.

A

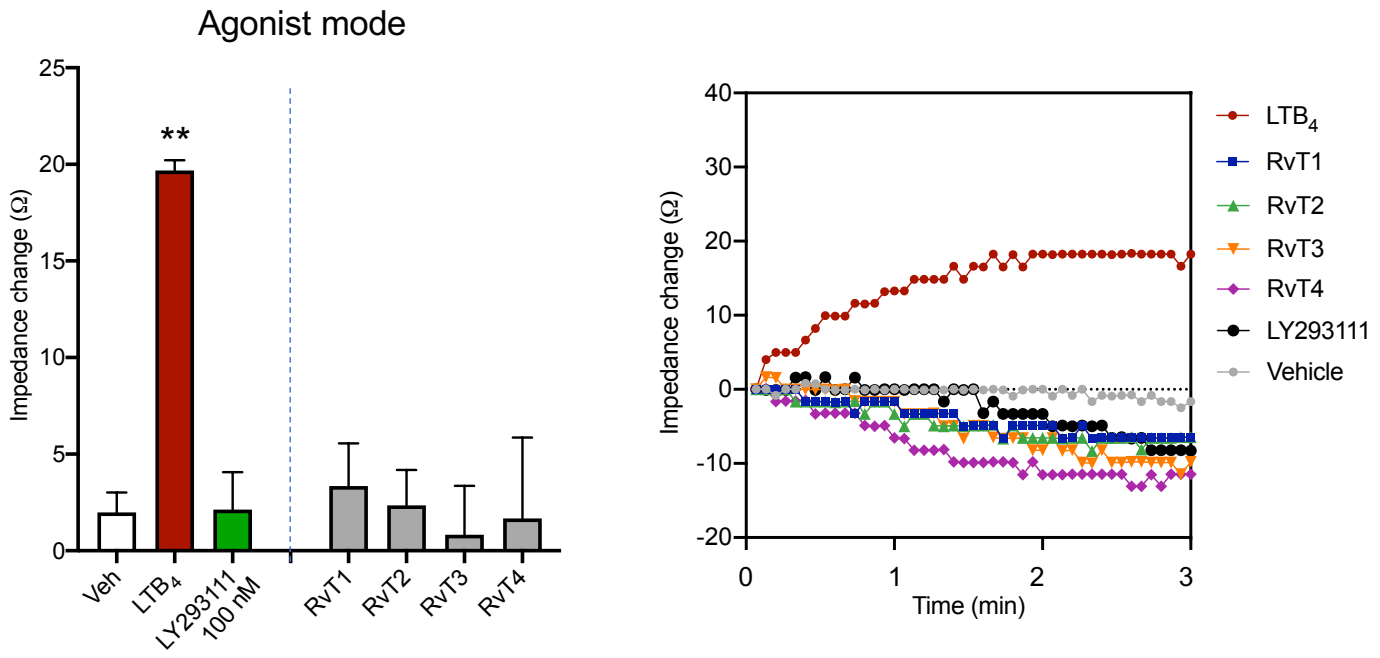

B

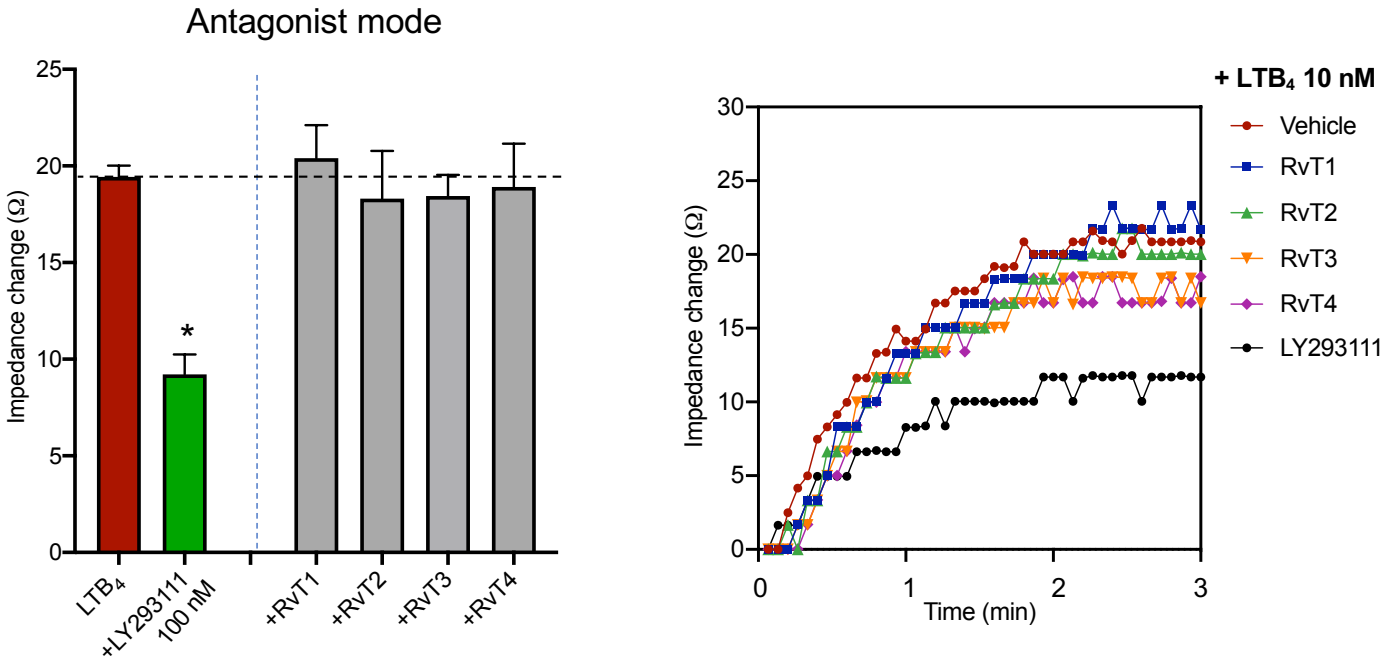

Figure S3. RvTs do not activate or antagonize LTB_4 signals with human recombinant BLT1 receptor *in vitro*

Ligand-receptor interactions were monitored by measuring impedance changes in cultured CHO-hBLT1 cells using an ECIS system (Applied Biophysics). Cells were plated (1×10^5/well in 8-well chamber slides), (A) incubated with vehicle, LTB_4, RvT1, RvT2, RvT3, RvT4 (10nM) or a BLT1 antagonist (LY293111; 100 nM) for 10 min, followed by (B) addition of 10 nM LTB_4 for 10 min. (A,B) Results are (left panels) impedance changes; mean±SEM; n = 3 independent experiments, and (right panels) real-time tracings from a representative experiment. (A) **P<0.01 vs veh, LY293111, RvT1, RvT2, RvT3 and RvT4. (B) *P<0.05 vs LTB_4, LTB_4 +RvT1, LTB_4 +RvT2, LTB_4 +RvT3 and LTB_4 +RvT4; One-way ANOVA with Tukey multiple comparisons.

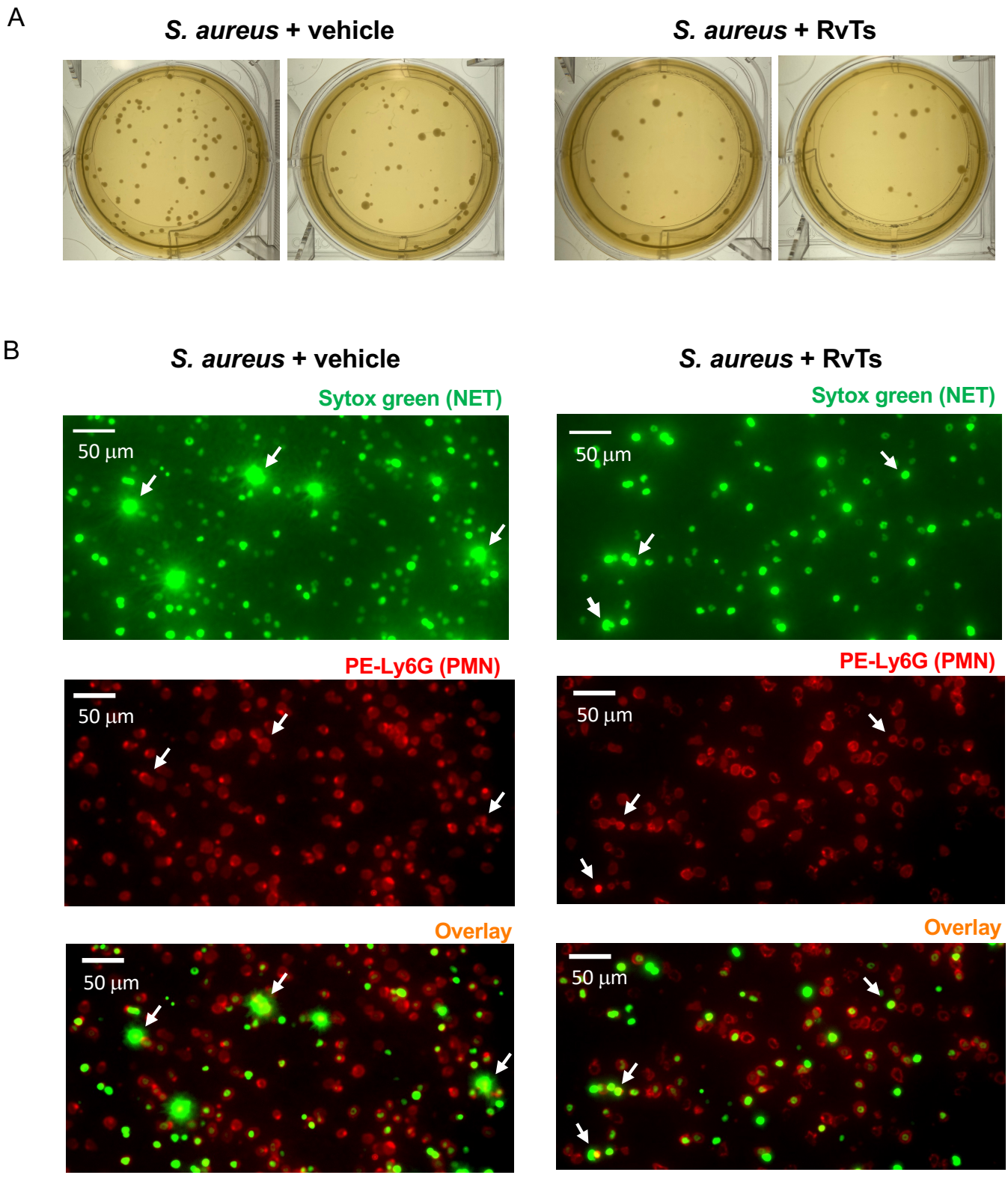

Figure S4. Bacterial titers and NETs from *S. aureus* infected mice
See Methods and figure legend of Figure 4 for experimental details.
(A) Representative images of bacterial titers from infectious exudates.
(B) Representative images of NETs in exudates collected from *S. aureus* infected mice with or without RvTs. Green: Sytox Green; Red: PE-labeled anti-Ly-6G Ab for mouse PMN. NETs are indicated by arrows. Scale bars: 50 μm.

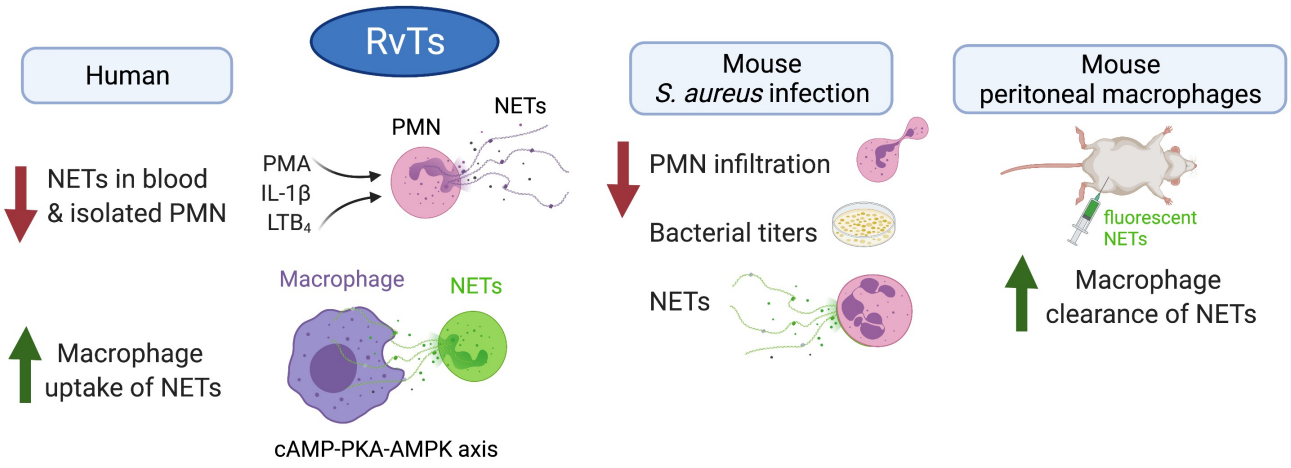

Figure S5. Schematic summary: Resolvin T-series reduce NETosis and enhance macrophage clearance of NETs.
RvTs reduced PMA-stimulated NETs in human blood, and IL-1β and LTB_4-stimulated NETs with isolated PMN. With human MΦ, RvTs enhanced NET ingestion via cAMP-PKA-AMPK axis. In mice, RvTs limited *S. aureus* dermal infection and stimulated peritoneal MΦ clearance of NETs.